
A.V. Simkin, A.V. Biryukov, N.I. Repnikov., O.N. Ivanov

Belgorod State National Research University,
85, Pobedy Str., Belgorod, 308015, Russia

**RELIABILITY TEST OF GENERATOR THERMOPILES MADE
WITH THE USE OF ARC PLASMA SPRAYING METHOD**

Long term test of generator thermopile samples for temperature cycling on their heat spreaders was performed. Depending on the number of cycles, changes in the basic technical characteristics of modules were traced and analyzed: electric power under optimal load, internal resistance and electromotive force (EMF) of thermopiles on achievement of design temperature difference. According to test results, amendments were introduced into thermopile manufacturing technique.

Key words: generator thermopiles, reliability, temperature cycling, characteristics of thermopile, mechanical destruction.

Introduction

Performance reliability of a thermoelectric generator (TEG) is defined as the probability of failure-free operation of installation for a specified time, for instance, its service life. In assessing the suitability and prospects, especially of self-contained thermoelectric installation, reliability is a prime consideration, as long as failure of independent marine or space power generation system can have grave consequences [1].

The basic structural unit of any TEG defining service life, time to failure and to a great degree the cost of the entire device is a thermoelectric module consisting of generator thermopiles. TEGs generally comprise tens and hundreds of generator thermopiles and even a greater number of junctions and connections each of which can cause TEG malfunction.

Heating and cooling of thermoelements can create large temperature gradients on contact layers of legs, hence, mechanical stresses causing formation of cracks, lamination and other thermoelectric material damages. It can drastically increase contact electric resistance and, thus, reduce the power and efficiency of thermoelements [1].

The purpose of this work was to study the reliability of a generator thermopile, where connection of basic elements, i.e. semiconductor legs, was done by arc plasma spraying method. Reliability was determined by carrying out long term test of generator thermopile samples for temperature cycling on heat spreaders. All samples under study were made by a unified technique. In so doing, the design employed semiconductor legs of bismuth telluride obtained by zone recrystallization and powder metallurgy methods. The reasons for a change in the basic technical characteristics of a generator thermopile in the course of the test were investigated.

Experimental procedure and samples

To perform the experiment, small lots of samples (4–5 pcs of each type) of generator thermopiles of the type TGB-P-NT-6 were made with extruded legs and TGB-P-NT-8 with the legs obtained by zone melting and hot pressing methods.

Design of generator thermopile samples is similar to that of thermopiles 7.5/2.5, described in [2], but has a variety of improvements (see Fig. 1).

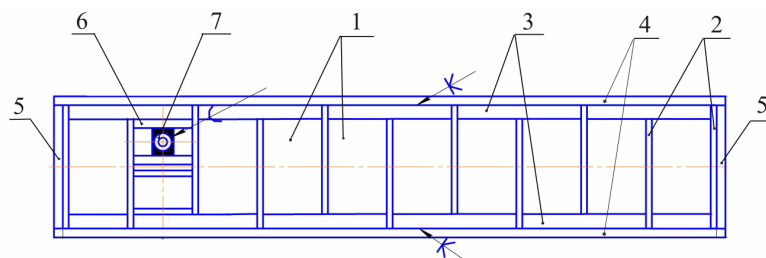


Fig. 1. Schematic of TGB-P-NT in section: 1 – thermoelement; 2 – glass fiber laminate cartridge; 3 – metal coating (subconnecting and connecting layers); 4 – ceramic heat spreaders; 5 – insulation coating; 6 – electric contact; 7 – electric wire.

Averaged values of technical characteristics of samples as compared to thermopile prototype 7.5/2.5 [2] are represented in Table 1.

Table 1

Technical characteristics of a generator thermopile

Thermopile designation	–	№ 1	№ 2	№ 3
Thermopile marking by manufacturer	Thermopile 7.5/2.5 according to [2]	TGB-P-NT-6 legs extrusion	TGB-P-NT-8 legs zone melting	TGB-P-NT-8 legs pressing
Dimensions of thermopile, mm	67 × 78.5 × 8.5	57 × 78 × 9	57 × 78 × 11	57 × 78 × 11
Number of thermocouples	83	68	68	68
Dimensions of legs, mm	5 × 5 × 6	5 × 5 × 6	5 × 5 × 8	5 × 5 × 8
Electric power, W	7.5	8.0	6.0	7.0
Optimal load voltage, V	2.5	2.0	2.05	2.3
Hot side operating temperature, °C	305	300	300	300
Cold side operating temperature, °C	100	100	100	100
Internal resistance, Ω	≤ 0.35	0.26	0.34	0.37

Temperature fields in a generator thermopile are directly related to the emergence of mechanical stresses due to the difference in thermal expansion coefficients of elements forming the thermopile rigid structure. Such thermal stresses lead to the appearance of cracks, violation of contacts and, as a consequence, destruction of thermoelectric device. These effects depend to a large extent on the properties of thermoelectric materials [1].

In a generator thermopile, a thermoelement is not a mechanically free system, being almost always related to other structural elements (base, heat-exchanger, etc). The thermoelement cannot freely change its shape with temperature variation, and this deformation constraint is the reason for origination of internal stresses, so if special measures are not taken, the value of these stresses can exceed permissible values and lead to thermoelement destruction. The less is thermoelement height, the stronger the leg semiconductor is bent (the radius of curvature is smaller) [3], the larger are the

arising mechanical stresses, hence, the higher the probability of thermoelement destruction and generator thermopile failure.

Such assertions are confirmed by practical test results: [2] describes drastic increase in the internal resistance (in fact, failure) of thermopile 7.5/2.5 (leg height 6 mm) after performing 40 – 70 cyclic temperature variations on the heat spreaders of this type of a generator thermopile.

The authors also obtained rather modest results when performing cycling tests on thermopiles of the type TGB-P-NT-6 (leg height 6 mm) with the legs made by zone melting and pressing methods: the thermopiles lost more than 5 % of generated electric power at the end of no more than 100 cycles.

To perform cyclic life test, installation shown in Fig. 2 was made.



Fig. 2. Picture of installation for life test of plane-type generator thermopile.

The installation enables test to be performed on three generator thermopiles independently. Each of three thermopiles is clamped between the heater which allows creating and maintaining the hot side temperature of up to 450 °C and the cooler which allows maintaining the cold side temperature of a generator thermopile from 30 °C to 100 °C. The accuracy of temperature control on the cooler and heater is not worse than ± 2 °C, temperature spread on the area of the cooler and heater is no more than 1 °C. The temperature is controlled by three thermocouples located at different points on the cold side and two thermocouples on the hot side. The thermocouples caulked in the heater and cooler are adjacent directly to thermopile heat spreaders. Control of heater power and electromagnetic valves of coolers is done after a program from personal computer connected to the installation. According to experimental procedure, temperature on thermopile heat spreaders was varied in conformity with a cyclogram shown in Fig. 3.

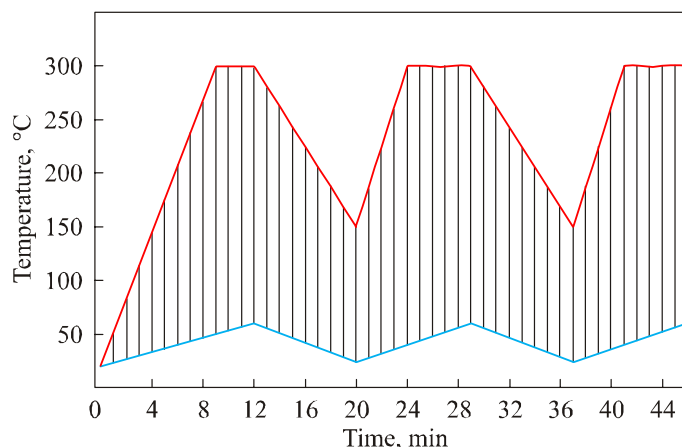


Fig. 3. Plot of temperature change on the thermopile heat spreaders when performing the tests: red colour shows temperature variation on the hot side, and blue colour – on the cold side.

When fixing a generator thermopile between the heater and cooler, the thermopile electric wires are connected to installation “Load unit”. On switching test performance program, the generator thermopile hot side is heated to a temperature of $T_h = 300 \pm 2$ °C. When this temperature is reached, it is maintained until the cold side temperature rise and equalization to $T_c = 60 \pm 2$ °C. Upon reaching said temperatures, the “Load unit”, in conformity with a program, measures current-voltage characteristic of the generator thermopile at $\Delta T = 240$ °C. The resulting current-voltage characteristic data with a serial number of cycle performed are written into a file.

On completion of current-voltage characteristic measurement, the heater is switched off and cooling half-cycle is carried out to the hot side temperature 150 ± 2 °C. In so doing, the cold side temperature drops to 25...30 °C. In the course of heating and cooling processes, there is current flow through the thermopile. For this period the “Load unit” sets the resistance corresponding to optimal load value at given ΔT . When setting test parameters, the optimal load value is set by the operator. The range of current-voltage characteristic measurement and the number of points in it is also assigned by the program. The entire temperature cycle of heating and cooling does not exceed 17 minutes for thermopile of the type TGB-P-NT-6. Fig. 4 shows a typical volt-ampere characteristic obtained on the generator thermopile life test installation upon reaching the assigned ΔT .

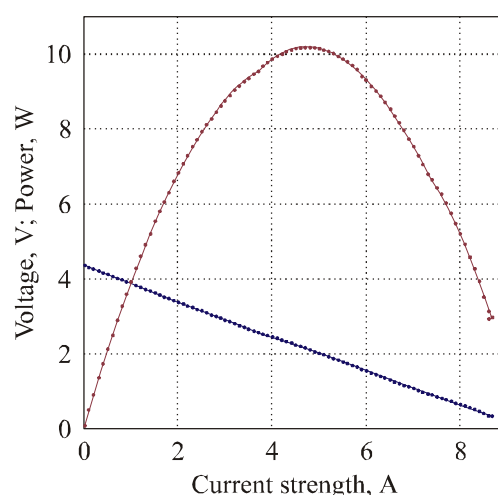


Fig. 4. Current-voltage characteristic of thermopile № 2 obtained on life test installation: $T_h = 300$ °C, $\Delta T = 240$ °C, red colour shows a change in power, blue – a change in voltage versus current value.

Results and discussion

By the results of preliminary test of TGB-P-NT-6 made with the legs produced by zone melting and pressing, it was decided to use these materials for making thermopiles of the type TGB-P-NT-8 with the leg height 8 mm. Potentially, thermopiles with higher legs are more reliable [3]. From the beginning, stable characteristics in the course of long duration test (over 600 cycles) were exhibited by thermopile №1 with extruded legs.

Fig. 5 shows a plot of power versus the number of thermocycles for generator thermopile samples under study.

Each point on the plot in Fig. 6 corresponds to EMF value (maximum value of voltage in the absence of current see in Fig. 4) measured at cyclogram point, when the hot side temperature $T_h = 300$ °C, $\Delta T = 240$ °C.

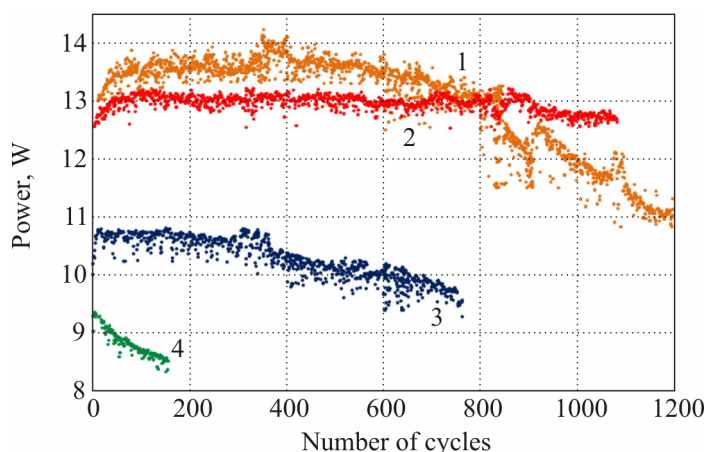


Fig. 5. Plot of change in maximum power at $T_h = 300\text{ }^\circ\text{C}$, $\Delta T = 240\text{ }^\circ\text{C}$ generated by TGB-P-NT samples in the course of test for temperature cycling on heat spreaders. Thermopile: 1 – № 1 extrusion; 2 – № 1-M extrusion; 3 – № 2 zone melting; 4 – № 3 pressing.

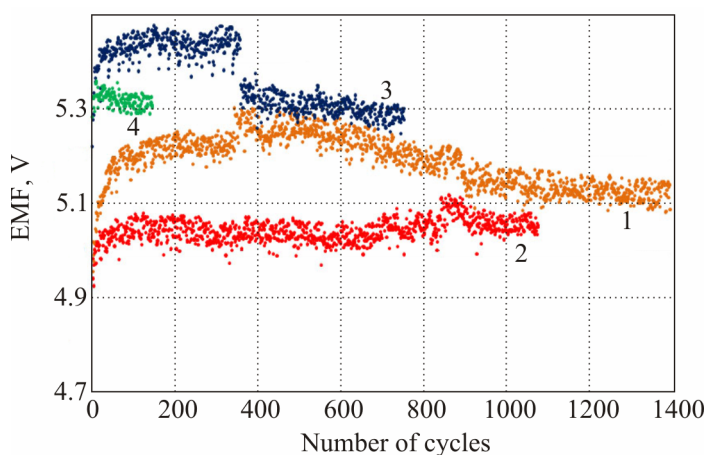


Fig. 6. Plot of change in the EMF of generator thermopile samples at $T_h = 300\text{ }^\circ\text{C}$, $\Delta T = 240\text{ }^\circ\text{C}$ in the course of test for temperature cycling on heat spreaders. Thermopile: 1 – № 1 extrusion; 2 – № 1-M extrusion; 3 – № 2 zone melting; 4 – № 3 pressing.

It is known [1, 4, 5] that the electric power of a generator thermopile:

$$W = E_{II} \cdot I = \frac{E^2 \cdot R}{(R + r)^2}, \quad (1)$$

where

$$E_{II} = (T_h - T_c) \cdot \alpha_a - I \cdot r = \Delta T \cdot \alpha_a - I \cdot r \quad (2)$$

– on-load voltage output;

$$E = (T_h - T_c) \cdot \alpha_a \quad (3)$$

– voltage between the electric wires of open generator thermopile, i.e. EMF; R – electric resistance of net load; r – internal resistance of a generator thermopile proper with the assigned

$$\Delta T = T_h - T_c; \quad (4)$$

T_h , T_c – the generator thermopile hot and cold side temperatures, respectively;

$$\alpha_a = \frac{1}{T_h - T_c} \cdot \int_{T_c}^{T_h} \alpha_{1,2}(T) dT; \quad (5)$$

where $\alpha_{1,2}(T)$ is the Seebeck coefficient function of temperature characterizing the properties of leg material [1, 4, 5].

Each point of the plot shown in Fig. 5 was obtained on condition of maximum power, i.e. when $R = r$ [1]. Thus, maximum power of a generator thermopile given to net load can reach

$$W = \frac{E^2}{4r}. \quad (6)$$

From (6) it is seen that the main characteristic which is of concern to generator thermopile end users and TEG designers, namely maximum power (Fig. 5) given to net load, is a function of EMF (Fig. 6) and the internal resistance of a generator thermopile.

Scatter of points with close values of cycle number on the plots depicted in Figs. 5 and 6 is related to the error in maintenance and reproduction of ΔT and the error proper in measuring voltage and current in the circuit.

Analyzing the plots, one can make the following conclusions: for thermopiles № 1 and № 1-M with extruded legs and № 2 during the initial stage of testing (the first 50 – 70 cycles) there is growth of maximum power due to growth of EMF of thermopiles, which in turn from (3) can be due to growth of “real” temperature difference ΔT on the junctions of thermoelectric elements, i.e. due to a decrease in thermal resistance on the generator thermopile heat spreaders. Besides, EMF increase during this stage can be related to growth of the Seebeck coefficient α of legs material due to cycling-caused temperature annealing of semiconductor material as part of operating thermopile.

Temperature variation along thermoelement leg creates thermal stresses in material. Thermal stresses are also caused by nonuniform temperature fields at points of heat supply and removal that can bring about large losses of heat flow which in the general case must pass in heat pipeline, through electrical insulation, connecting buses between thermoelectric element legs and numerous junctions and contacts between them. Temperature gradient losses in this case can reach considerable values and have a pronounced effect on the efficiency of thermoelectric element [1].

For thermopile № 3 there was no considerable growth of maximum power in cycling. On the contrary, as in the case of TGB-P-NT-6 with the legs of this material and zone melted legs, there was a smooth reduction of maximum power without considerable change in EMF. Power drop is related to considerable growth of thermopile internal resistance: prior to testing the internal resistance of thermopile, measured at room temperature was 0.37 Ω , and after performing 160 temperature cycles – 0.45 Ω .

Characteristics of thermopile № 2 were relatively stable up to 366 thermal cycle, following which EMF was drastically reduced by 0.1 V. Analysis of generator thermopile after removal from testing showed cracking and lamination of ceramic heat spreader in one of the angles on the hot side of the thermopile. In this angle, heat flow through thermoelements was violated with local overheat of connections on the hot side. The situation was worsened by local overheat of this area due to increased Joule heat release. All this accelerated the process of generator thermopile destruction (internal resistance growth) in the course of subsequent thermal cycles. Prior to testing, the internal resistance of thermopile measured at room temperature was 0.361 Ω , and after performing 765 temperature cycles – 0.407 Ω .

Temperature difference on the generator thermopile heat spreaders leads to origination of static and dynamic mechanical stresses on its structural members. In so doing, cyclic thermal, hence mechanical

effects on module structural members, namely compression, expansion and bending, can result in mechanical stresses exceeding the ultimate strength of materials forming part of a generator thermopile. Fatigue of materials during cyclic mechanical effects is the reason for thermopiles destruction [6].

Evident destruction of thermopile № 1 with the legs of extruded material began after 830 thermal cycles. Maximum power started falling relatively drastically, though EMF was reduced rather slowly. From (6) it follows that power drop is due to internal resistance increase. Prior to testing, the internal resistance of thermopile measured at room temperature was 0.26Ω . After performing 830 temperature cycles – 0.31Ω . By the end of generator thermopile testing (after 1620 cycles) the internal resistance of thermopile was 0.47Ω and it continued generating 10.4 W of maximum power. Thermopile № 1 was removed from testing, and from its legs arranged along the perimeter a thermoelement was withdrawn for thorough analysis of changes that occurred. This thermoelement was used to make a lateral microsection. The resistance of this sample prior to and after mechanical exposure did not change.

The lateral microsection of thermoelement was investigated with the use of optical microscope OLYMPUS GX51 with 1000 x magnification. Scanning electron microscope (SEM) Quanta 200 3D was used to study sample morphology (see Fig. 7) in secondary electrons mode (SE) and back-scattered electrons mode (BSE). Elemental analysis carried out by X-ray spectral microanalysis with the use of energy-dispersive spectrometer EDAX has shown that defects 4 and 5 in Fig. 7 are gas-filled cavities.

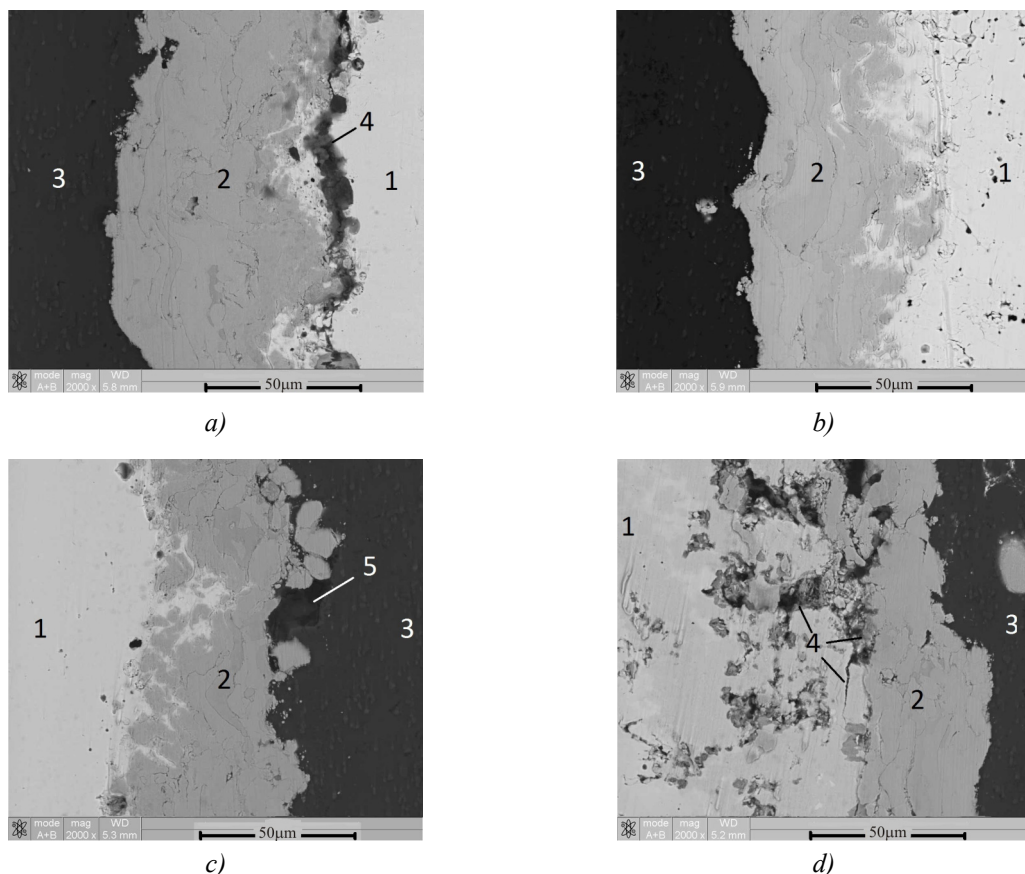


Fig. 7. SEM-image of transient layers of near-contact region of legs on the cold (a and b) and hot (c and d) side of thermoelement sample: 1 – semiconductor leg of bismuth telluride (extrusion), 2 – barrier layer of subconnection, 3 – connection layer of aluminium alloy, 4 – destructions (cracks, laminations, etc), 5 – pores in connection layer of aluminium alloy created at spraying.

The obtained results of generator thermopile testing allowed amending the technique of arc-plasma spraying of barrier and connection layers of thermopile thermoelements. According to amended technology, a sample of thermopile № 1-M with extruded legs was made. The sample was tested for temperature cycling on heat spreaders by the same procedure. Test results are also shown in Figs. 5 and 6. Prior to testing, the thermopile internal resistance measured at room temperature was 0.26 Ω , and after performing 1085 temperature cycles – 0.275 Ω .

Based on the results of [6], it can be supposed that, while under temperature difference, the thermopile acquires the shape of elliptical paraboloid, which leads to growth of mechanical shear stresses in thermoelement junctions with increase in element coordinate with respect to the geometric centre of thermopile. Displacement of elements at the corners of module is the greatest [6]. Dependence of deformation value of thermopile surfaces is a linear function of temperature difference.

Earlier, in [7], the authors carried out a series of mechanical tests of semiconductor bismuth telluride legs prepared by different methods. Maximum values of breaking load under shear load were obtained exactly on the legs produced by extrusion and zone melting (thermopiles № 1 and № 2). As long as destruction caused by mechanical stresses occurs mainly in semiconductor material in the immediate vicinity of connecting layers and in semiconductor-barrier layer junction, the resistance of leg material to shear mechanical loads is not the least of the factors. Of crucial importance is also the presence and depth of damaged layers on the surface of leg connecting planes [7-11].

Conclusions

1. It is established that generator thermopiles with semiconductor legs of low-temperature material bismuth telluride, connected by arc plasma spraying technique, are resistant to temperature cycling on heat spreaders and are capable of withstanding over 1000 temperature cycles from 300 °C to 150 °C on the hot side and from 60 °C to 20 °C on the cold side of thermopile with heating and cooling cycle duration not more than 17 minutes. In so doing, the basic technical characteristics of thermopile, namely electric power, internal resistance and EMF are not reduced more than by 5 %.
2. Thermopiles made by arc plasma connection technique, with higher legs, are potentially more resistant to temperature cycling on heat spreaders than thermopiles with the same legs, but of lower height.
3. Under the conditions of temperature difference, mechanical shear stresses are originated in the thermopile, leading to destructions mainly in semiconductor material in the immediate vicinity of connecting layers and in semiconductor-barrier layer junction. Destructions appear both on the cold side and the hot side. Maximum destructions are originated in thermoelements located in a series of legs along the perimeter of thermopile, with maximum mechanical stresses created in the corners of the thermopile.

The work was performed under the financial support of Foundation for Promotion of the Development of Small Forms of Enterprises in Science and Technology, Government contract №8095p / 12669 of 18.06.2010, the financial support of Ministry of Education and Science of Russian Federation, with the use of instrument base of Centre for Collective Use of Scientific Equipment “Diagnostics of structure and properties of nanomaterials” at Belgorod State National Research University.

References

1. A.S. Okhotin, *Thermoelectric Generators*, Ed. by A.P. Regel (Moscow: Atomizdat, 1971), 288 p.
2. A.A. Pustovalov, V.V. Gusev, L.P. Nebera et al., ATEG Based Power Sources for Autonomous

- Automated Systems and Technical Facilities Controlling the State of Gas Mains and the Work of Gas Wells, *J. Thermoelectricity* 4, 65 – 71 (1998).
3. E.G. Pokorny, A.G. Scherbina, *Calculation of Semiconductor Cooling Devices* (Leningrad, Nauka Publishers Leningrad Division., 1969), 206 p.
 4. A.I. Burstein, *The Physics of Calculation of Semiconductor Thermoelectric Devices* (Moscow: State Publishing House of Physics and Mathematics Literature, 1962), 135 p.
 5. O.V. Marchenko, A.P. Kashin, V.I. Lozbin, and M.Z. Maksimov, *Methods for Calculation of Thermoelectric Generators* (Novosibirsk: Nauka. RAS Siberian Publishing Company, 1995), 222 p.
 6. A.V. Solovyova, S.V. Bobzhenko, and P.S. Krokhin, Thermoelectric Module Strains Under Electric Current Flow, *J. Thermoelectricity* 1, 71 – 74 (2009).
 7. A.V. Simkin, A.V. Biryukov, N.I. Repnikov et al., Reliability Enhancement of Generator Thermopiles Assembled Through Use of Interconnects by Arc Plasma Spraying Method, *Proceedings of XIII Interstate Workshop "Thermoelectrics and their Application"* (Saint-Petersburg, 2012), 540 p.
 8. A.V. Biryukov, N.I. Repnikov, O.N. Ivanov, et al., Advantages of Using the Electric Erosion Cutting and Flame Spraying at Connection of Thermoelements Based on Extruded Bismuth Telluride, *J. Thermoelectricity* 3, 36 – 42 (2011).
 9. A.V. Simkin, A.V. Biryukov, N.I. Repnikov et al., Effect of Contact Surface Condition on the Adhesion Strength of Interconnect Layers of Thermoelements Based on Extruded Bismuth Telluride, *J. Thermoelectricity* 2, 13 – 19 (2012).
 10. V.B. Osvensky, V.V. Karatayev, N.V. Mal'kova et al., Diffractometric Study of Structural Mechanisms of Adhesion Failure of Anti-Diffusion Nickel Coating on *Bi-Te-Se* Thermoelectric Materials, *J. Surface Investigation. X-ray, Synchrotron and Neutron Techniques* 3, 95 – 98 (2001).
 11. V.B. Osvensky, V.V. Karatayev, N.V. Mal'kova et al., Study of Structural Mechanisms of Adhesion Failure of Anti-Diffusion Nickel Coating on *Bi-Sb-Te* Thermoelectric Materials, *Materials of Electronic Technics*, 70-73 (2002).

Submitted 11.04.2013.